Dynamic Simulation and Experimental Evaluation of EPDM Synthesis with $Et(Ind)_2ZrCl_2$/MAO Catalyst System

MÔNICA CARCUCHINSKI HAAG,[1] JOÃO HENRIQUE ZIMNOCH DOS SANTOS,[1] JAIRTON DUPONT,[1] ARGIMIRO RESENDE SECCHI[2]

[1] Instituto de Química, Universidade Federal do Rio Grande do Sul, Av. Bento Gonçalves, 9500-91540-000, Porto Alegre, RS, Brazil

[2] Depto. de Engenharia Química, Universidade Federal do Rio Grande do Sul, Rua Luiz Englert, s/n-90040-040, Porto Alegre, RS, Brazil

Received 5 April 1999; accepted 15 June 1999

ABSTRACT: A mathematical model for the homogeneous terpolymerization of ethylene–propylene–diene (EPDM) in a semibatch reactor using $Et(Ind)_2ZrCl_2$/MAO as a catalyst system was developed and reported herein. In this study, we developed a kinetic model in order to explain the catalyst and EPDM properties such as catalyst activity, weight-average molecular weight, and terpolymer composition, which were experimentally and theoretically obtained. For this system, a lower E/P feed ratio leads to a lower molecular weight and a broader initial molecular weight distribution, while the increase in diene concentration leads to a decrease in the catalyst activity without broadening the MWD of the resulting polymers. The proposed model accounts for these experimental trends and for some data in the literature. © 2000 John Wiley & Sons, Inc. J Appl Polym Sci 76: 425–438, 2000

Key words: metallocene; EPDM; modeling; olefin terpolymerization

INTRODUCTION

Metallocene catalysts have become increasingly important as α-olefin polymerization catalysts. The single-site metallocene/methylaluminoxane (MAO) system combines high activity with the possibility of tailoring polymer properties.[1] Depending on the metallocene ligands and symmetry, these catalysts permit a strong control of the regio- and stereoregularities and of the molecular weight distribution (MWD) of homopolymers, as well as the synthesis of copolymers with narrow MWDs, narrow chemical composition distribution (CCD), and higher activities. The disadvantages of this systems are the high Al/Zr ratios (1000–5000) necessary to achieve stability and good activity.

The copolymers of ethylene and propylene (EP) are of great industrial interest. These EP polymers show elastic properties and, together with 2–5 wt % of dienes as third monomers, they constitute a family of terpolymers: the ethylene–propylene–diene monomer (EPDM). Since there are no double bonds in the backbone of the polymer, it is less sensitive to oxidation reactions. The EPDMs available from industry are mostly based on 2-ethylidenebi-cyclo[2.2.1]hept-5-ene (ENB).[2] For both technical and economical reasons, these termonomers are incorporated in E/P chains only in very low limited proportions (<2 mol %).

In most technical processes for the production of EPDM rubber, vanadium-based catalyst systems, such as $VOCl_3$ or $VO(OR)_3$, cocatalyzed by alkylaluminum chloride in the presence of or-

Correspondence to: J. H. Z. dos Santos (jhzds@if.ufrgs.br).

Journal of Applied Polymer Science, Vol. 76, 425–438 (2000)
© 2000 John Wiley & Sons, Inc.

ganic halogen promoters have been currently employed. However, such catalyst systems present a drastic loss in catalyst productivity in the presence of dienes, as well as chain branching and crosslinking in the course of the terpolymerization.[3] Moreover, even organoaluminum cocatalysts are capable of reducing the active V (III) species to the inactive V (II) ones. This loss in productivity leads to a higher residual vanadium content, which must not exceed 10 ppm to avoid coloring, aging, and toxicity.[4]

Similar elastomers, but less colored, have been obtained with metallocene/MAO catalysts at a much higher activity,[5–7] leading, consequently, to a lower residual metal content.[8] It seems that, contrarily to what takes place in the case of vanadium-based catalysts, metallocenes show stability toward the diene deactivation reaction.[9] Projections for metallocene-catalyzed EPDM demand is about 5×10^5 tons/year within 10 years. This value, although small, is significant for this product and illustrates that metallocenes are facilitating the penetration of hydrocarbon polymers into areas currently served by high-cost engineering thermoplastics.[10]

The $Et(Ind)_2ZrCl_2$/MAO catalyst system is by far the most studied metallocene system in the open literature for the production of polyethylene, polypropylene, EP copolymers, and EPDM terpolymers. In EP copolymerizations, this *ansa*-metallocene catalyst incorporates larger amounts of propylene than do nonbridged systems and, as a consequence, produce lower molecular weights.[11,12]

In a previous work,[13] we developed a model to describe the terpolymerization reaction of EPDM using vanadium-based catalysts. The model was used to study the influence of the Al/V ratio and diene concentration on the weight-average molecular weight, on the polydispersity index, and on the terpolymer composition. For high diene concentrations, the fit concerning the influence of diene concentration on the yield of a polymer did not agree very well and this behavior was attributed to side reactions (such as crosslinking) which were not taken into account in the model. These side reactions might take place due to the acid character of vanadium catalysts which promote crosslinking reactions by activating the nonpolymerizable diene double bond.

In the case of metallocene catalysts, the influence of the diene is not thoroughly understood. There is a higher comonomer incorporation than that in the case of the vanadium catalysts. However, the activity falls with increase in the diene concentration as in the case of vanadium catalysts.[9]

In the present work, the model proposed by Haag et al.[13] is extended to study the influence of the reaction conditions on the terpolymer properties using 2-ethylidenebi-cyclo[2.2.1]hept-5-ene (ENB) as the diene and the $Et(Ind)_2ZrCl_2$/MAO *ansa*-metallocene as the catalyst system. The proposed kinetic mechanisms presented in the literature concern mainly copolymerization reactions and there is a lack of studies dealing with a kinetic mechanism of EPDM terpolymerization by metallocenes. To better understand the dynamic behavior of this catalyst system, we built a kinetic model based on our experimental results and on some evidence cited in the literature.

EXPERIMENTAL

Chemicals

Polymerization-grade ethylene and propylene were purchased from White-Martins (Porto Alegre, Brazil) and dried using molecular sieve (0.4 nm) columns. Toluene was dried by refluxing over metallic sodium, followed by distillation under an argon atmosphere. 2-Ethylidenebicyclo[2.2.1]hept-5-ene (ENB), the catalyst precursor $Et(Ind)_2ZrCl_2$ (Witco, Mechelen, Belgium), and the cocatalyst MAO (supplied by Witco, 10.0 wt % toluene solution, 1.7 Al wt % as TMA, average molar mass 900 g mol^{-1}) were used without further purification.

Polymerization Reactions

The scheme of the polymerization reactor was reported elsewhere.[13] The polymerizations were carried out in a 2-L glass reactor (Büchi) using toluene as a solvent. The diene, the cocatalyst, and the required amount of the catalyst were introduced in this order into the reactor containing toluene (1 L) under positive pressure of a mixture of ethylene and propylene. The temperature was maintained at 313 K, under a continuous flow of ethylene and propylene, for 60 min. The reaction was then quenched by the addition of ethanol (at room temperature). The polymer was collected, washed with ethanol (1 L), and vacuum-dried at room temperature for several hours.

Polymer Characterization

The polymer films were characterized by infrared spectroscopy (Bomem FTIR spectrophotometer) measuring the ratio of the intensities of the 1155 cm^{-1} methyl band and the 720 cm^{-1} methylene band to determine the ethylene and propylene content, according to ASTM D3900. The diene incorporation was monitored by infrared spectroscopy[13] and ^{1}H-NMR analysis using a Varian-300 MHz equipment at 353 K. The samples were dissolved in *o*-dichlorobenzene and benzene-d_6 (20 v/v).

The transition temperatures (T_g and T_m) of the polymers were determined using differential scanning calorimetry (12000 PL-DSC) with a heating rate of 20 K min^{-1}, while the GPC measurements (GPC, Waters 150) were made at 413 K using 1,2,4-trichlorobenzene as a solvent and polystyrene calibration curves.

UV/Visible Experiments

The reactor precontact conditions were simulated in an experimental apparatus similar to that described by Coevoet et al.[14] This apparatus permitted us to perform all studies using UV/visible spectroscopy under an inert atmosphere.

The Al/Zr total ratio and catalyst concentration were reduced in order to keep the Beer's Law linearity at the concentration range. The Zr/diene molar ratio was kept at the same ratio as was used for the polymerization runs. The UV/visible analyses were performed in a Shimadzu spectrophotometer in the 300–600-nm wavelength range using a quartz cell (1.0-cm path length).

THE TERPOLYMERIZATION MODEL

The use of models to describe polymerization reactions are growing in interest since they allow one to better understand the experimental observations when a great number of reaction parameters are involved. Copolymerization and terpolymerization models employing soluble Ziegler–Natta catalyst systems were previously discussed elsewhere.[13]

Concerning the metallocene catalyst, a few models have been proposed in the literature. Hoel et al.[15] developed an EP copolymerization model using supported-metallocene systems devoted to explain the unexpected broad CCD with this single-site catalyst. Based on experimental and theoretical results, these authors concluded that the breadth of the CCD was a consequence of monomer mass-transport limitations during the polymer particle granules' growth.

Soares and Hamielec[16] developed a generic model to describe copolymerization reactions, using Ziegler–Natta or metallocene catalysts, which could predict MWDs and copolymer compositions, taking into account the existence of multiple types of active sites for homogeneous and heterogeneous E–P copolymerization. These authors made a very interesting discussion about monomer diffusivity at low and at high reactivities and their influence on the polydispersity index, on the molecular weight, and on the chemical composition. The chain-length and chemical-composition distributions were obtained from the Stockmayer equation.[17] In a subsequent article, this model was extended to a series of continuous-stirred tank reactors (CSTR).[18] Concerning the terpolymerization kinetic model for the metallocene catalyst, there are a few reports in the literature,[6] and in the following, a kinetic model based on the commonly accepted mechanisms of homo- and copolymerization reactions for metallocene systems is discussed.

KINETIC MODEL AND KINETIC CONSTANT PARAMETER ESTIMATION

The generic kinetic mechanism for the present model is shown in the Appendix. In the following, each reaction step is discussed, in order to account this generic model to the case in study. In the catalyst-activation reaction (k_a), the metallocene is transformed in an alkylated active species, Zr–CH_3 (C_2), resulting from chlorine abstraction by an MAO cocatalyst followed by alkylation using MAO or trimethylaluminum (TMA) present in MAO itself. It is worth mentioning that the role of MAO as a cocatalyst is not still clearly elucidated and many functions have been attributed to this compound in the literature. Besides alkylation of the catalyst,[19,20] other functions such as stabilization of the cationic metallocenic alkyl species by acting as a counterion and the prevention of bimolecular reduction of the catalyst[19,21,22] have also been proposed. Moreover, aluminoxanes are also capable of scavenging impurities such as water and oxygen from the reaction milieu.[19] There is a minimum Al/Zr rate which is necessary to produce stable active species, and for higher Al/Zr rates, the system achieves stability toward a max-

imum activity.[14] During the polymerization reactions, another type of active species, Zr—H (also C_2), can also be generated through β-elimination. In our model, we did not distinguish the alkylated from the hydride active species.[23]

In Figure 1, we can see the EPDM yield of the $Et(Ind)_2ZrCl_2$/MAO catalyst system along with the terpolymerization reaction. For comparative reasons, data from the vanadium-based catalyst[13] obtained under the same diene concentration and similar productivity but different E/P feed ratio and catalyst concentration were included. According to experimental data and to the theoretical curve, the metallocene system does not achieve the end of the polymerization in 30 min of reaction time due to the constant regeneration of active species either by β-elimination or by a chain-transfer reaction. On the other hand, in the case of vanadium-based systems, as already mentioned, the deactivation step by diene presents a relevant kinetic constant (10^4 mol L^{-1} min^{-1}), which is much higher than that for metallocene (10^1 mol L^{-1} min^{-1}). Moreover, the absence of the β-elimination reaction contributes also to achieving the polymerization end in about 15 min of reaction time, as we can observe in Figure 1.

Concerning the deactivation by the diene, we have included in Table I both the possibility of the catalyst (kx_3C_1) and active species (kx_3C_2) deactivation. As we could not distinguish between the two deactivation mechanisms, under our experiential conditions, we assumed the same value for both constants, which are fitted to the polymerization yield under different initial diene concentrations. This assumption will be better discussed later, taking into account UV/visible experiment results. The chain-initiation reaction with ethylene was considered higher than that with propylene due to the higher reactivity of the former, being in accordance with other models for copolymerization with α-olefin proposed in the literature.[24]

Concerning the chain propagation constants, the best fitting was obtained including six possibilities of monomer combination. The possibilities of combining diene–propylene (k_{32}), propylene–diene (k_{23}), and diene–diene (k_{33}) were excluded since there is no diene–propylene copolymerization reported in the literature and also the possibility of diene–diene (k_{33}) due to the low probability of the reaction occurring in the terpolymerization system. The propagation reaction through propylene–propylene (k_{22}) was assumed by several authors[24–26] to be the lowest propagation constant for copolymerization reactions, considering the lower activity for the homopolymerization with this higher α-olefin and the decrease of the molecular weight increasing the α-olefin concentration in the feed.

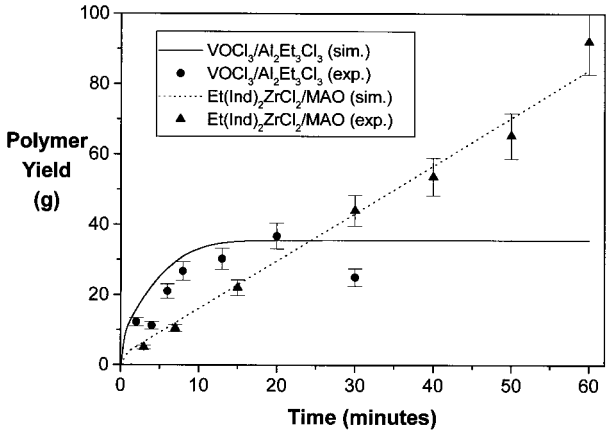

Figure 1 Comparison of metallocene and vanadium-based catalyst systems for EPDM production. [ENB] = 1.8×10^{-3} mol L^{-1}; $VOCl_3$ = 2.32×10^{-4} mol L^{-1} (n-hexane); Al/V = 8.3; E/P = 25/75, 298 K; $Et(Ind)_2ZrCl_2$ = 1.0×10^{-5} mol L^{-1} (toluene); Al/Zr = 3000; E/P = 40/60, 313 K.

The chain-transfer reactions can occur preferentially by β-H elimination, followed by transfer to ethylene and to propylene monomers and to MAO. The β-H elimination reaction has been proposed as the main-chain termination mechanism for metallocene catalysts and this reaction leads, in the case of ethylene, to vynil chain ends.[23] Moreover, C—H bond activation has been proposed as a termination mechanism where the olefin is inserted in an M—R bond in a different orientation from that of the propagation step, generating, therefore, an alkane and a vynil monomer.[27] Concerning the chain transfer by the monomers, recently, D'Agnillo et al.[28] proposed that chain-transfer reactions to ethylene might take place in ethylene homopolymerization with the zirconocene-based systems. However, through chain-end analysis, Naga et al.[25] stated that copolymers of ethylene and propylene mainly terminate with EP and PP sequences. For simplification, we will consider in the present system only a monomer transfer reaction to propylene.

Ruchatz and Fink[29] very recently discussed the possibility of chain transfer of a chain terminated with norbornene during ethylene–norbornene copolymerization with metallocene catalysts and

Table I. Kinetic Constants for Homo- and Copolymerization Models Proposed in the Literature and for This Model

Reaction Step	Constant (mol L^{-1} min^{-1})	Hoel and Cozewith[a]	Chien[b]	Chien[c]	Beigzadeh et al.[d]	Present Model[e]	Adjusting Parameters
Activation	k_a[f]					4.0×10^1	—
Deactivation							
Catalyst	k_{x3C1}					8.0×10^1	Concn $[\Delta M_3(0)]$
Active species	k_{x3C2}					8.0×10^1	Concn $[\Delta M_3(0)]$
Chain							
Initiation							
Ethylene	k_{y1}				2.4×10^6	5.0×10^4	—
Propylene	k_{y2}				6.0×10^5	5.0×10^3	—
Chain							
Propagation							
Ethylene	k_{11}	9.1×10^4	6.62×10^4		2.4×10^6	1.0×10^6	F_1, concn, M_w
	k_{12}	1.4×10^4	2.6×10^4		6.0×10^5	1.0×10^5	F_1, concn, M_w
	k_{13}					9.5×10^4	F_1, F_3, concn, M_w
Propylene	k_{21}	9.8×10^3	6.1×10^4		2.1×10^6	2.8×10^5	F_1, concn, M_w
	k_{22}	1.6×10^3	2.4×10^4		5.3×10^5	5.0×10^3	F_1, concn, M_w
	k_{23}					0.0	—
Diene	k_{31}					4.6×10^3	F_1, F_3, concn, M_w
	k_{32}					0.0	—
	k_{33}					0.0	—
Chain							
transfer							
Propylene	k_{tr12}					6.0	F_1, M_w $[\Delta y_{ET}/y_{PP}(0)]$
	k_{tr22}					6.0	F_1, M_w $[\Delta y_{ET}/y_{PP}(0)]$
	k_{tr32}					0.0	—
Ethylene	k_{tr11}, k_{tr21}, k_{tr31}					0.0	—
Al–alkyl	$k_{trAl(1,2,3)}$[f]		1.1×10^{-1}	7.2×10^{-1}		0.0	—
β-Hydride	$k_{\beta 1}$			1.7×10^1	0.6	1.8×10^1	M_w
Elimination	$k_{\beta 2}$				0.6	1.8×10^1	M_w
	$k_{\beta 3}$					0.5	M_w $[\Delta M_3(0)]$
Chain							
termination							
Catalyst deactivation	$k_{t(1,2,3)}$[f]					0.0	—

[a] Metallocene system, ref. 15.
[b] $Et(Ind)_2ZrCl_2$, ref. 12.
[c] Ethylene homopolymerization/$(Cp)_2ZrCl_2$, ref. 21.
[d] Ethylene-1-octene copolymerization, ref. 27.
[e] $Et(Ind)_2ZrCl_2$.
[f] min^{-1}.

excluded the possibility of β-H elimination or chain transfer to a monomer due to sterical hindrance. These authors took into account only transfer reactions by C—H activation. It was also observed that by increasing the cyclic olefin content in the reaction medium the copolymer molecular weight increases at the expense of the activity. Based on these results and on our experimental data, we assumed a lower kinetic constant value for transfer reactions with living chains ended by diene units.

The occurrence of β-CH_3 elimination normally takes place with metallocene-containing substituted Cp* systems. As we used $Et(Ind)_2ZrCl_2$ as a catalyst, such a possibility was also neglected in the present model. The branching reactions concerning the remaining double bond of ENB were not taken into account since it is hindered and might be hardly incorporated by the $Et(Ind)_2$-$ZrCl_2$/MAO system.

The employed kinetic constants were dynamically estimated from experimental data using the

gPROMS Estimation Tool.[30] This estimation was concomitantly done with the choice of the best kinetic mechanism to describe the terpolymerization reactions.

The determination of the polymerization rate constants is not a trivial task. For copolymerization systems, there are well-established methodologies such as the Fineman–Ross method[31] and the Kelen–Tüdös[32] method for the determination of the reactivity ratios. In the case of terpolymers, there is not a thoroughly accepted methodology yet.

We used our model to estimate these constants and this was done by fitting the experimental data concerning the catalyst activity, weight-average molecular weight, polydispersity index, and chemical composition of the samples collected during the polymerization. The estimated kinetic constants as well as the main related adjusting parameters used for the estimation are shown in Table I. For comparative reasons, some kinetic constants presented in the literature to similar systems were also included.

THE MODEL EQUATIONS

The model was developed using the same assumptions made in our previous study.[13] The reactor was operated in a semibatch mode. The gas phase was continuously fed to avoid change in the gas composition, while the liquid phase was operated in the batch mode. The mass balance for the gas phase was done under the same considerations as in our previous model. The presence of a single active species and the usually proposed kinetic mechanisms for metallocene polymerization present in the literature were assumed in the mass balance for the liquid phase. In the following, the equations which describe the mass balance for the liquid phase are presented, and they are based on the general kinetic model described in the Appendix. Some of those reactions will be later neglected by choosing the zero value to the kinetic constant.

Mass Balance for liquid phase
Catalyst species

$$\frac{dD}{dt} = (k_x + k_{x3C1}M_3)C_1 + k_{x3C2}M_3C_2 + k_{t1}P^0 + k_{t2}Q^0 + k_{t3}R^0 \quad (1)$$

$$\frac{dC_1}{dt} = -(k_x + k_{x3C1}M_3 + k_a)C_1 \quad (2)$$

$$\frac{dC_2}{dt} = k_aC_1 - k_{y1}C_2M_1 - k_{y2}C_2M_2 - k_{x3C2}C_2M_3 + k_{\beta1}P^0 + k_{\beta2}Q^0 + k_{\beta3}R^0 + k_{trAl1}AlP^0 + (k_{trAl2}Al + k_{\beta CH3})Q^0 + k_{trAl3}AlR^0 \quad (3)$$

$$\frac{dAl}{dt} = -k_{trAl1}AlP^0 - k_{trAl2}AlQ^0 - k_{trAl3}AlR^0 \quad (4)$$

Monomers

$$\frac{dM_1}{dt} = kla(M_{1EQ} - M_1) - (k_{y1}C_2 + k_{11}P^0 + k_{21}Q^0 + k_{31}R^0 + k_{tr11}P^0 + k_{tr21}Q^0 + k_{tr31}R^0)M_1 \quad (5)$$

$$\frac{dM_2}{dt} = kla(M_{2EQ} - M_2) - (k_{y2}C_2 + k_{12}P^0 + k_{22}Q^0 + k_{32}R^0 + k_{tr12}P^0 + k_{tr22}Q^0 + k_{tr32}R^0)M_2 \quad (6)$$

$$\frac{dM_3}{dt} = -(k_{13}P^0 + k_{23}Q^0 + k_{33}R^0 + k_{x3C1}C_1 + k_{x3C2}C_2)M_3 \quad (7)$$

Polymer species with i = *1*

$$\frac{dP_1}{dt} = k_{y1}C_2M_1 + k_{tr11}M_1P^0 + k_{tr21}M_1Q^0 + k_{tr31}M_1R^0 - P_1(\alpha + k_{11}M_1) \quad (8)$$

$$\alpha = (k_{\beta1} + k_{tr11}M_1 + k_{trAl1}Al + k_{t1} + (k_{tr12} + k_{12})M_2 + k_{13}M_3) \quad (9)$$

$$\frac{dQ_1}{dt} = k_{y2}C_2M_2 + k_{tr12}M_2P^0 + k_{tr22}M_2Q^0 + k_{tr32}M_2R^0 - Q_1(\beta + k_{22}M_2) \quad (10)$$

$$\beta = (k_{\beta2} + k_{\beta CH3} + k_{trAl2}Al + k_{t2} + k_{tr22}M_2 + (k_{tr21} + k_{21})M_1 + k_{23}M_3) \quad (11)$$

Zeroth-order moments for the living chains

$$\frac{dP^0}{dt} = k_{y1}C_2M_1 + k_{tr11}M_1P^0 + k_{tr21}M_1Q^0 + k_{tr31}M_1R^0 + k_{21}M_1Q^0 + k_{31}M_1R^0 - P^0\alpha \quad (12)$$

Table II. Simulation Parameters and Initial Conditions Used in the Theoretical Model

Parameters	Values	Initial Conditions	Values
P_{SET} (bar)	1.5	$C_1(0)$ (mol L^{-1})	1.0×10^{-5}
T_{SET} (K)	313.0	Al/Zr	3000
$kla_{PP} = kla_{ET}$ (min^{-1})	0.4	$M_1(0)$ (mol L^{-1})	0.06723
$\overline{\Delta H_P}$ (cal mol^{-1})	1.0×10^4	$M_2(0)$ (mol L^{-1})	0.28442
A_M (m^2)	0.1072	$M_3(0)$ (mol L^{-1})	1.8×10^{-3} to 5×10^{-1}
V_C (L)	0.9	$P_T(0)$ (bar)	1.50
$V_L = V_G$ (L)	1.0	$T(0)$ (K)	313.0
		$y_{ET}/y_{PP}(0)$	80/20; 40/60

$$\frac{dQ^0}{dt} = k_{y2}C_2M_2 + k_{tr12}M_2P^0 + k_{tr22}M_2Q^0 + k_{tr32}M_2R^0 + k_{12}M_2P^0 + k_{32}M_2R^0 - \beta Q^0 \quad (13)$$

$$\frac{dR^0}{dt} = k_{13}P^0M_3 + k_{23}Q^0M_3 - R^0\gamma \quad (14)$$

$$\gamma = (k_{trAl3}Al + k_{\beta 3} + k_{t3} + (k_{tr32} + k_{32})M_2 + (k_{31} + k_{tr31})M_1) \quad (15)$$

Zeroth-order moments for the dead chains

$$\frac{dU^0}{dt} = (P^0 - P_1)\eta_1 + (Q^0 - Q_1)\eta_2 + R^0\eta_3 \quad (16)$$

$$\eta_1 = (k_{trAl1}Al + k_{\beta 1} + k_{t1} + k_{tr11}M_1 + k_{tr12}M_2) \quad (17)$$

$$\eta_2 = (k_{trAl2}Al + k_{\beta 2} + k_{t2} + k_{tr21}M_1 + k_{tr22}M_2 + k_{\beta CH3}) \quad (18)$$

$$\eta_3 = (k_{trAl3}Al + k_{\beta 3} + k_{t3} + k_{tr31}M_1 + k_{tr32}M_2) \quad (19)$$

Zeroth-order for total moments

$$S^0 = U^0 + P^0 + Q^0 + R^0 \quad (20)$$

The higher-order moments were calculated in the same manner as in our previous work,[13] and the mean theoretical weight- and number-average molecular weight ($\overline{M_W}$ and $\overline{M_N}$) as well as and the polydispersity index ($\overline{PDI}$) were calculated through the method of moments using the following assumption:

$$w = F_1Mw_1 + F_2Mw_2 + F_3Mw_3 \quad (21)$$

where F_1, F_2, and F_3 are the theoretical molar fractions of the incorporated monomers in the polymer chain and Mw_1, Mw_2, and Mw_3 are the monomer molecular weights:

$$\overline{M_W} = w\,\frac{S^2}{S^1} \quad (22)$$

$$\overline{M_N} = w\,\frac{S^1}{S^0} \quad (23)$$

$$\overline{PDI} = \frac{\overline{M_W}}{\overline{M_N}} \quad (24)$$

This approach was earlier proposed by McAuley et al.[33] to calculate the M_w for ethylene-1-butene copolymers and we have already used this assumption in good agreement with the experimental data.[13]

Ideal behavior was assumed for both the gas and liquid phases. The ideal gas law was used to describe the gas phase, while Henry's law was used to calculate the solubility of the monomers in the solvent.[34]

The system of 30 differential equations was solved by the gPROMS simulation software.[30] In Table II, some of the parameters and initial conditions used in the simulation and experimental runs are presented.

RESULTS AND DISCUSSION

In Figure 2, we can see the weight-average molecular weight and the ethylene molar fraction as function of the reaction time obtained at high E/P feed ratio (80/20). We can see that the maximum of the molecular weight is achieved in the first

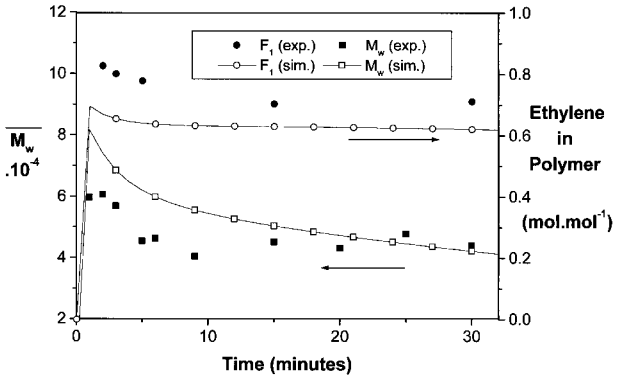

Figure 2 Weight-average molecular weight and ethylene molar fraction during terpolymerization. [ENB] = 1.8×10^{-2} mol L^{-1}; $Et(Ind)_2ZrCl_2$ = 1.0×10^{-5} mol L^{-1} (toluene); Al/Zr = 3000, E/P = 80/20, 313 K.

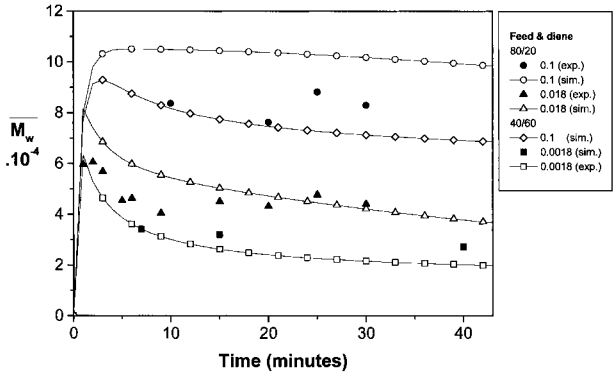

Figure 3 Weight-average molecular weight for different diene concentrations and E/P feed ratios. $Et(Ind)_2ZrCl_2$ = 1.0×10^{-5} mol L^{-1} (toluene); Al/Zr = 3000, 313 K.

minutes of the reaction time as a consequence of greater ethylene incorporation. We can also observe that the proposed kinetic mechanism takes into account this behavior at the beginning of the reaction which depends on the initial conditions as we will see in the following figures. As we can see, the steady-state hypothesis may not be valid for these initial moments, and in this case, a dynamic approach seems to be more suitable.

A similar heterogeneity in chemical composition during the reaction was observed by Hoel et al.[15] using a supported conventional metallocene catalyst on EP copolymerization and they attributed this behavior to mass-transfer resistance. Using a metallocene catalyst with a more *open* geometry, this heterogeneity was not observed. The control of these initial transient behaviors can be made by the proper choice of operational conditions, prepolymerization reactions, and catalyst-support treatment.[35]

Influence of the E/P Feed Ratio

Figure 3 shows the influence of the E/P feed ratio and of the ENB concentration on the EPDM weight-average molecular weight. The increase of propylene in the feed decreases the molecular weight as a consequence of the lower propylene chain propagation kinetics (k_{21}, k_{22}) and the higher chain-transfer reactions with propylene (k_{tr12}, k_{tr22}). Besides increasing diene concentration, the molecular weight increases under both E/P feed conditions due to the high incorporation of the higher molar mass monomer and to the lower transfer termination reaction with the chain terminated with diene.

The polydispersity index increases for higher propylene amounts in the gas feed, mainly in the beginning of the reaction, as we can observe in Figure 4. This broadening of MWD for lower E/P feed ratios was already experimentally reported for EP copolymerization with this catalyst system and the authors attributed this fact to the existence of two types of active sites under these conditions.[11] However, there are many discussions in the literature concerning the reasons for MWD broadening, mainly concerning mass-transfer resistance or the existence of multiple active sites. With these so-called single-site catalysts, the existence of multiple active species can be a consequence either of lower Al/Zr ratios[14] or of two types of alkyl aluminum as cocatalysts,[29] which are not the case here. Mass-transfer resis-

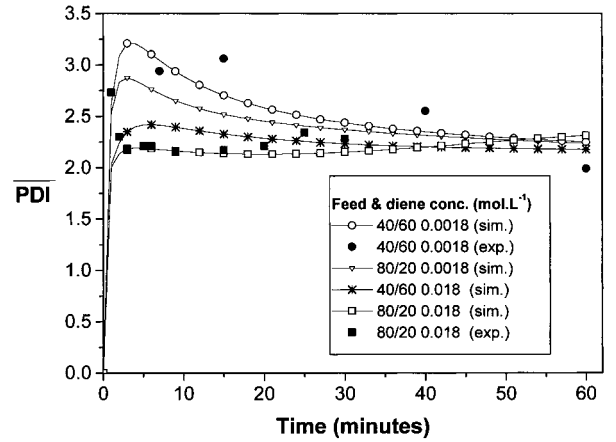

Figure 4 Polydispersity indexes for different diene concentrations and E/P feed ratios. $Et(Ind)_2ZrCl_2$ = 1.0×10^{-5} mol L^{-1} (toluene); Al/Zr = 3000, 313 K.

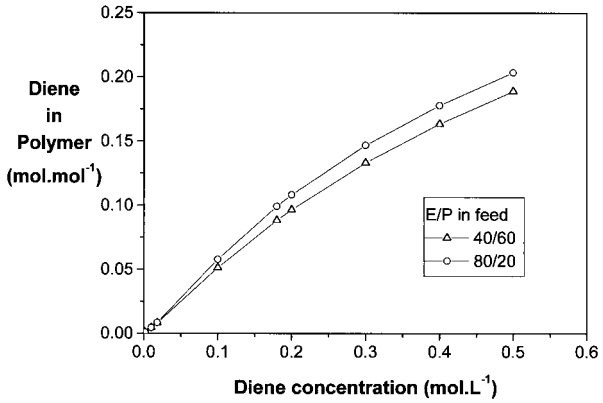

Figure 5 Diene molar fraction in polymer for different initial diene concentrations and E/P feed ratios. $Et(Ind)_2ZrCl_2 = 1.0 \times 10^{-5}$ mol L^{-1} (toluene); Al/Zr = 3000, 313 K.

tance has been pointed as one reason for MWD broadening due to the high activity of these catalysts.[29] In our system, this broadening seems to be related to mass-transfer resistance caused by the high sensitivity of the molecular weight to change in the feed composition and the high reactivity for incorporation of ethylene compared to propylene.

We can also see that under the same E/P feed ratio the increase of the ENB concentration lowers the initial polydispersity index. A similar effect was reported by Soares and Hamielec,[16] studying the mass-transfer resistance by simulating the decrease of the number of active sites in propylene homopolymerization. They observed in dynamic simulation that the increase of the number of active sites leads to a higher initial polydispersity index and as the reaction proceeds the polydispersity index tends to the most probable value. We can also observe in Figure 4 that according to our proposed kinetic model the number of active sites is lowered by increase of the diene concentration, which leads to a decrease of the initial polydispersity index under the same E/P feed ratio.

With the proposed propagation constants, it is possible to obtain the theoretical diene incorporation versus the initial diene concentration curve, as shown in Figure 5. In accordance with experimental data obtained by Malmberg,[7] there is not a considerable change in the diene incorporation in changing the E/P feed ratio.

Influence of the Diene Concentration

To better understand the effect of diene on the deactivation process, we monitored the effect of diene concentration in the active species formation by UV/visible experiments. Figure 6(a) shows the UV-vis spectra of a toluene solution containing $Et(Ind)_2ZrCl_2$ and MAO. The presence of a large band centered at 455 nm characterizes the presence of active species. As observed by Coevoet et al.[14] the introduction of α-olefins to this system leads to a hypsochromic shift (425 nm), indicating its coordination to the active ionic species. As the reaction proceeds, a decrease in the maximum of absorbance of the band related to the active species is also observed.[21] In the present system, we can also verify a similar behavior when ENB is introduced to the catalyst $Et(Ind)_2ZrCl_2$ [Fig. 6(b)]. According to these results, we can conclude that the deactivation can occur either over the active species or over the catalyst.

In Figure 7, we can see the influence of the diene concentration on the polymer yield after 30

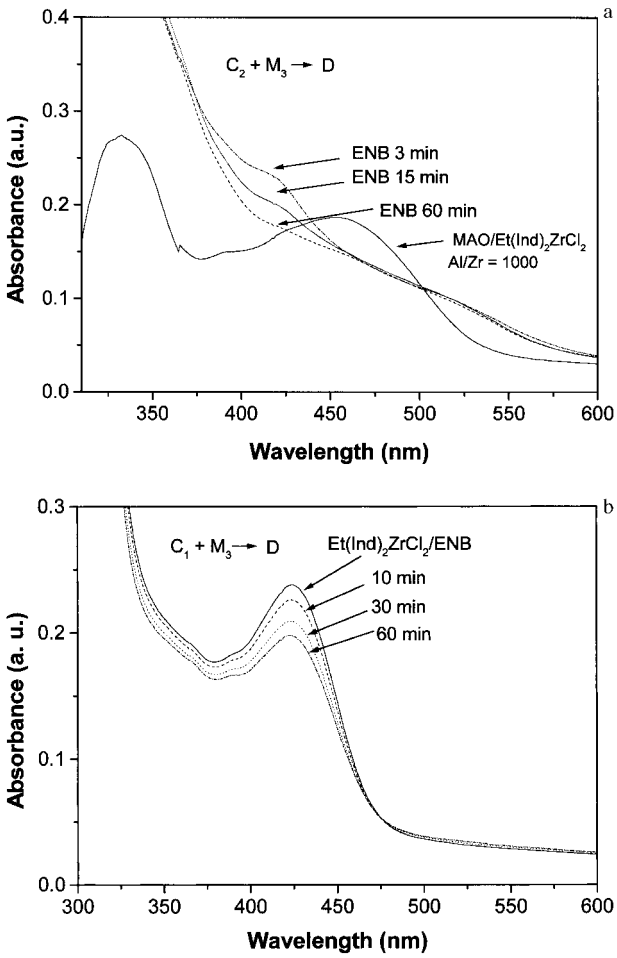

Figure 6 U.V./visible spectra for diene in presence of (a) formed active species and (b) catalyst. $Et(Ind)_2ZrCl_2 = 1.0 \times 10^{-4}$ mol L^{-1} (toluene); Al/Zr = 1000, 298 K; Zr/ENB = 1.0×10^{-3}.

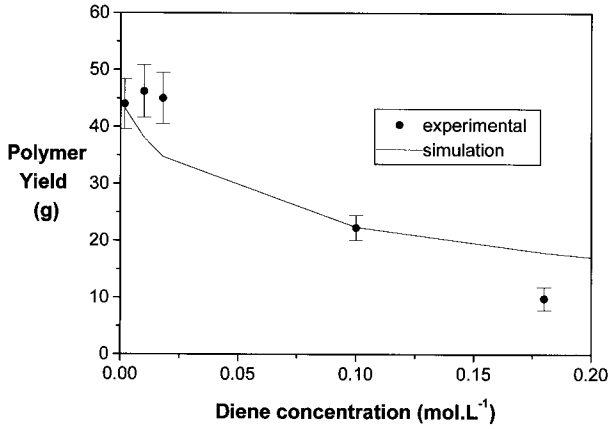

Figure 7 Polymer yield after 30 min of terpolymerization at different diene concentrations. $Et(Ind)_2ZrCl_2$ = 1.0×10^{-5} mol L^{-1} (toluene); Al/Zr = 3000; E/P = 80/20, 313 K.

min of reaction time. At low diene concentrations, there might be a competition between active species deactivation and the propagation reaction, both promoted by diene. Thus, under such experimental conditions, no significant change can be observed in the activity. On the other hand, for higher diene concentrations, the activity falls probably due to the deactivation mechanism promoted by the diene, which prevails over the active species.

In the case of vanadium-based catalysts, decrease in the activity with increase of the diene concentration is due to the reduction of the vanadium(III) active species to the vanadium(II) inactive ones. Concerning the deactivation of the metallocene active species, recently Bergström et al.[36] observed decrease of the activity in the ethylene and norbornene copolymerization under high cyclic olefin concentrations. For the $Me_2Si(Ind)_2$-$ZrCl_2$/MAO system, the same authors observed a more accentuated effect when compared to the $Et(Ind)_2ZrCl_2$/MAO system. This effect was attributed to the deactivation of the metallocene active species by norbornene. This negative comonomer effect related to styrene was also pointed out by Sernetz and Mülhaupt[37] in the terpolymerization of ethylene, 1-octene, and styrene.

By the simulation results, we observed that for a higher diene concentration (0.2–0.5 mol L^{-1}), the catalyst activity curve decays more monotonously. A similar trend was also experimentally observed by Malmberg and Löfgren[7] between a similar diene concentration range.

According to Table III, as the diene concentration is increased from 10^{-2} to 10^{-1} mol L^{-1}, the weight-average molecular weight increases, while the polydispersity index remains practically constant. This is evidence that under these experimental conditions there are no side reactions leading to crosslinking and this model is still valid for such a diene concentration. It is worth noting that under similar high diene concentrations the polymer produced with vanadium-based catalysts are completely crosslinked.

Concerning EPDM production with metallocene catalysts, there are different points of view for the diene influence on the ethylene incorporation. Dolatkhani et al.,[9] using a lower E/P feed ratio, found a slight decrease in the ethylene content with increase of the diene concentration (range 0.1–0.5 mol L^{-1}) and these authors attributed this behavior to a change on the active site after diene incorporation. Chien and He,[6] working with lower diene concentrations and using different polymerization procedures, found different trends related to the E/P ratio in the diene incorporation.

According to our experimental data and simulation results for ethylene and propylene incorporation, the tendency of the diene incorporation follows the same trend as the ethylene content (Fig. 8 and Table III) in the case of lower diene concentrations. However, for higher diene concentrations, it is possible to observe through the sim-

Table III. Polymer Properties for Different Diene Concentrations at 30 min: $Et(Ind)_2ZrCl_2$ = 1.0×10^{-5} mol L^{-1}, Al/Zr = 3000, E/P = 80/20, 313 K

Diene (mol L^{-1})	Ethylene (mol %)	Diene (mol %)	$M_w \times 10^{-4}$ (amu)	PDI	T_g (K)	T_m (K)
0	89.0	0.0	5.6	2.2	—	353.1
1.0×10^{-2}	76.9	0.1	5.3	2.4	—	350.0
1.8×10^{-2}	75.7	0.2	4.4	2.3	228.3	—
1.0×10^{-1}	79.3	2.9	7.4	2.6	268.9	—
1.8×10^{-1}	82.5	2.8	7.4	2.1	291.8	—

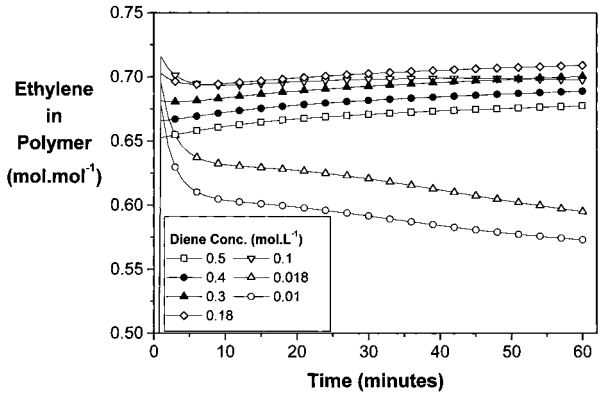

Figure 8 Ethylene molar fraction in EPDM during the polymerization for different initial diene concentrations. $Et(Ind)_2ZrCl_2 = 1.0 \times 10^{-5}$ mol L^{-1} (toluene); Al/Zr = 3000; E/P = 80/20, 313 K.

ulation results the decrease in the ethylene incorporation between the diene concentration of 0.18 and 0.50 mol L^{-1}. This behavior agrees with the results of Malmberg and Löfgren[7] who observed, using this same catalyst system in EPDM synthesis, a decrease in ethylene incorporation when the diene concentration was increased from 0.1 to 0.6 mol L^{-1}. These experimental and theoretical results for high diene concentrations are not straightforward with the assumption that there is no coupling with diene–propylene, but probably this is caused by the different reactivities of these two monomers related to ethylene. The proposed kinetic mechanism takes into account these behaviors. To improve the accuracy of this kind of model, it is necessary to create a methodology for the kinetic constant estimation for terpolymers, which are shown to be very sensitive.

CONCLUSIONS

With the proposed terpolymerization model, we were able to study the influence of different polymerization conditions on EPDM properties along the polymerization reaction. The general behavior of the obtained simulation results agrees not only with our experimental data, but also with other results from the literature, explaining polymer properties resulting from changes in the gas feed and in the diene concentration.

Concerning the polymer yield, the model fits the experimental data well, showing the different behavior of the system depending on the diene concentration. For higher diene concentrations, there is a decrease in the polymer yield as a consequence of the deactivation process promoted by the diene. Concerning the branching reactions promoted by the free double bond of the diene, it seems unlikely in this metallocene system, since we did not observe an increase in the MWD with increase in the diene concentration. This simplified model (one active site, without the influence of temperature on the kinetic constants) was shown to be very useful to better understand this complex polymerization system and it helps us to design new experiments to account for the polymerization mechanism.

NOMENCLATURE

Al	alkylaluminum concentration (mol L^{-1})
C_1, C_2	catalyst and active species concentration (mol L^{-1})
D	deactivated species concentration (mol L^{-1})
F_1, F_2, F_3	molar fractions of the incorporated monomers, ethylene, propylene, and diene, in the polymer chain
$\overline{PDI}$	polydispersity index
kla	volumetric convective mass-transfer coefficient on liquid phase (min^{-1})
M_3	diene concentration (mol L^{-1})
M_{1EQ}, M_1	ethylene concentration at equilibrium and at liquid phase (mol L^{-1})
M_{2EQ}, M_2	propylene concentration at equilibrium and at liquid phase (mol L^{-1})
P_1, P^0	activated ethylene units and zeroth-order moment for live chains terminated with ethylene (mol L^{-1})
Q_1, Q^0	activated propylene units and zeroth-order moment for live chains terminated with propylene (mol L^{-1})
R^0	zeroth-order moment for live chains terminated with diene (mol L^{-1})
S^0, S^1, S^2	zeroth-, first- and second-order total moments (mol L^{-1})
U^0	zeroth-order moment for all dead chains (mol L^{-1})
V_C, V_G, V_L	jacket, gas-phase, and liquid-phase volume (L)

w	weighted molecular weight of theoretical monomer (g mol^{-1})
$\overline{M_N}$, $\overline{M_W}$	number- and weighted-average theoretical molecular weight (amu)
P_{SET}, P_T	set-point and total pressure (bar)
T_{SET}	temperature in the set-point (K)
$\overline{\Delta H_P}$	mean heat of polymerization (cal mol^{-1} K^{-1})
$\Delta y_{ET}/y_{PP}(0)$	parameter estimation under the variation of the initial feed condition
$\Delta M_3(0)$	parameter estimation under the variation of the initial diene concentration
A_M	heat-jacket area (m^2)
y_{ET}, y_{PP}	mass fraction of ethylene and propylene in the feed

APPENDIX

A generic reaction mechanism and reaction rates for a terpolymerization reaction with metallocene catalysts can be stated as follows:

Catalyst activation

$$C_1 \xrightarrow{k_a} C_2 \quad k_a C_1 \tag{A.1}$$

Catalyst and active species deactivation

$$C_1 \xrightarrow{k_x} D \quad k_d C_1 \tag{A.2}$$

$$C_1 + M_3 \xrightarrow{k_{x3C1}} D \quad k_{x3C1} C_1 M_3 \tag{A.3}$$

$$C_2 + M_3 \xrightarrow{k_{x3C2}} D \quad k_{x3C2} C_2 M_3 \tag{A.4}$$

Chain initiation

$$C_2 + M_1 \xrightarrow{k_{y1}} P_1 \quad k_{y1} C_2 M_1 \tag{A.5}$$

$$C_2 + M_2 \xrightarrow{k_{y2}} Q_1 \quad k_{y2} C_2 M_2 \tag{A.6}$$

Chain propagation

$$P_i + M_1 \xrightarrow{k_{11}} P_{i+1} \quad k_{11} M_1 P_i \tag{A.7}$$

$$P_i + M_2 \xrightarrow{k_{12}} Q_{i+1} \quad k_{12} M_2 P_i \tag{A.8}$$

$$P_i + M_3 \xrightarrow{k_{13}} R_{i+1} \quad k_{13} M_3 P_i \tag{A.9}$$

$$Q_i + M_1 \xrightarrow{k_{21}} P_{i+1} \quad k_{21} M_1 Q_i \tag{A.10}$$

$$Q_i + M_2 \xrightarrow{k_{22}} Q_{i+1} \quad k_{22} M_2 Q_i \tag{A.11}$$

$$Q_i + M_3 \xrightarrow{k_{23}} R_{i+1} \quad k_{23} M_3 Q_i \tag{A.12}$$

$$R_i + M_1 \xrightarrow{k_{31}} P_{i+1} \quad k_{31} M_1 R_i \tag{A.13}$$

$$R_i + M_2 \xrightarrow{k_{32}} Q_{i+1} \quad k_{32} M_2 R_i \tag{A.14}$$

$$R_i + M_3 \xrightarrow{k_{33}} R_{i+1} \quad k_{33} M_3 R_i \tag{A.15}$$

Chain transfer to monomers (ethylene and propylene)

$$P_i + M_1 \xrightarrow{k_{tr11}} U_i + P_1 \quad k_{tr11} M_1 P_i \tag{A.16}$$

$$Q_i + M_1 \xrightarrow{k_{tr21}} U_i + P_1 \quad k_{tr21} M_1 Q_i \tag{A.17}$$

$$R_i + M_1 \xrightarrow{k_{tr31}} U_i + P_1 \quad k_{tr31}M_1R_i \qquad \text{(A.18)}$$

$$P_i + M_2 \xrightarrow{k_{tr12}} U_i + Q_1 \quad k_{tr12}M_2P_i \qquad \text{(A.19)}$$

$$Q_i + M_2 \xrightarrow{k_{tr22}} U_i + Q_1 \quad k_{tr22}M_2Q_i \qquad \text{(A.20)}$$

$$R_i + M_2 \xrightarrow{k_{tr32}} U_i + Q_1 \quad k_{tr32}M_2R_i \qquad \text{(A.21)}$$

Chain transfer to MAO

$$P_i + Al \xrightarrow{k_{trAl1}} U_i + C_2 \quad k_{trAl1}AlP_i \qquad \text{(A.22)}$$

$$Q_i + Al \xrightarrow{k_{trAl2}} U_i + C_2 \quad k_{trAl2}AlQ_i \qquad \text{(A.23)}$$

$$R_i + Al \xrightarrow{k_{trAl3}} U_i + C_2 \quad k_{trAl3}AlR_i \qquad \text{(A.24)}$$

Chain transfer by β-H

$$P_i \xrightarrow{k_{\beta 1}} U_i + C_2 \quad k_{\beta 1}P_i \qquad \text{(A.25)}$$

$$Q_i \xrightarrow{k_{\beta 2}} U_i + C_2 \quad k_{\beta 2}Q_i \qquad \text{(A.26)}$$

$$R_i \xrightarrow{k_{\beta 3}} U_i + C_2 \quad k_{\beta 3}R_i \qquad \text{(A.27)}$$

Chain transfer β-CH_3

$$Q_i \xrightarrow{k_{\beta CH3}} U_i + C_2 \quad k_{\beta CH3}Q_i \qquad \text{(A.28)}$$

Chain termination

$$P_i \xrightarrow{k_{t1}} U_i + D \quad k_{t1}P_i \qquad \text{(A.29)}$$

$$Q_i \xrightarrow{k_{t2}} U_i + D \quad k_{t2}Q_i \qquad \text{(A.30)}$$

$$R_i \xrightarrow{k_{t3}} U_i + D \quad k_{t3}R_i \qquad \text{(A.31)}$$

REFERENCES

1. See, for example: (a) Kaminsky, W. J Chem Soc Dalton Trans 1998, 1413; (b) Kissin, Y. V.; Kleiner, V. I.; Stotskaya, L. L. In Polymers and Copolymers of Higher α-Olefins; Krentzel, B. A., Ed.; Hanser: Munich, 1997; Chapter 1, p 11; (c) Ewen, J. A. Sci Am 1997, May, 60.
2. Strate, G. V. In Encyclopedia of Polymer Science and Engineering; Mark, H. F.; Bikales, N. M.; Overberger, C. G.; Koschwitz, J. J., Eds.; Wiley: New York, 1973; p 522.
3. Soga, K.; Yanogihara, H.; Lee, D.-H. Makromol Chem 1998, 190, 37.
4. Datta, S.; De, S. K.; Kontos, E. G.; Wefer, J. M.; Wagner, P.; Vida, A. Polymer 1996, 37, 4865.
5. Kaminsky, W.; Miri, M. J Polym Sci Polym Chem Ed 1985, 23, 2151.
6. Chien, J. C. W.; He, D. J Polym Sci Part A Polym Chem 1991, 29, 1609.
7. Malmberg, A.; Löfgren, B. J Appl Polym Sci 1997, 66, 35.
8. Haag, M. C.; dos Santos, J. H. Z.; Stedile, F. C.; Dupont, J. Submitted for publication in J Appl Polym Sci.
9. Dolatkhani, M.; Cramail, H.; Deffieux, A. Macromol Chem Phys 1996, 197, 2481.
10. Montagna, A.; Burkhart, R. M.; Dekmezian, A. H. Chemtech 1997, Dec. 26.
11. Lehtinen, C.; Löfgren, B. Eur Polym 1997, 33, 115.
12. Chien, J. W.; He, D. J Polym Sci Polym Chem Ed 1991, 29, 1585.
13. Haag, M. C.; dos Santos, J. H. Z.; Dupont, J.; Secchi, A. R. J Appl Polym Sci 1998, 70, 1173.
14. Coevoet, D.; Cramail, H.; Deffieux, A. Macromol Chem Phys 1998, 199, 1451.
15. Hoel, E. L.; Cozewith, C.; Byrne, G. D. AIChE J 1994, 40, 1669.
16. Soares, J. B. P.; Hamielec, A. E. Polym React Eng 1995, 3, 261.
17. Stockmayer, W. H. J Chem Phys 1945, 13, 199.

18. Soares, J. B. P.; Hamielec, A. E. Polym React Eng 1996, 4, 153.
19. Ewen, J. A.; Elder, M. J.; Jones, R. L.; Curtis, S.; Cheng, H. N. In Catalytic Olefin Polymerization; Keii, T.; Soga, K., Eds.; Proceedings International Symposium, Tokyo, 1989; p 439.
20. Sinn, H.; Kaminsky, W.; Vomman, H.-J.; Woldt, R. Angew Chem Int Ed Engl 1980, 19, 390.
21. Chien, J. C. W.; Wang, B.-P. J Polym Sci A Polym Chem 1990, 28, 15.
22. See, for example: (a) Tait, P. J. T.; Watkins, N. D. In Comprehensive Polymer Science; Allen, G.; Bevington, J. C., Eds.; Pergamon: Oxford, 1989; p 533; (b) Chien, J. C. W.; Wang, B.-P. J Polym Sci A Polym Chem 1989, 27, 1539.
23. Huang, J.; Rempel, G. L. Prog Polym Sci 1995, 20, 459.
24. Beigzadeh, D.; Soares, J. B. P.; Hamielec, A. E. J Appl Polym Sci 1999, 71, 1753.
25. Naga, N.; Ohbayashi, Y.; Mizunama, K. Macromol Rapid Commun 1997, 18, 837–851.
26. Lee, D.; Yoon, K.; Park, J.; Lee, B. Eur Polym J 1997, 53, 447.
27. Woo, T. H.; Fan, L.; Ziegler, T. Organometallics 1994, 13, 2252–2261.
28. D'Agnillo, L.; Soares, J. B. P.; Penlidis, A. Macromol Chem Phys 1998, 199, 955.
29. Ruchatz, D.; Fink, G. Macromolecules 1998, 31, 4684.
30. (a) Pantelides, C. C. presented at the 5th World Congress of Chemical Engineering, San Diego, CA, July 1996; (b) Pantelides, C. C. presented at CHEMPUTERS EUROPE III, Frankfurt, Oct. 1996; (c) Barton, P. I.; Smith, E. M. B.; Pantelides, C. C. presented at the AIChE Annual Meeting, Los Angeles, Nov. 1991.
31. Fineman, M.; Ross, S. D. J Polym Sci 1950, 5, 269.
32. Kelen, T.; Tüdös, F. J Macromol Sci-Chem A 1975, 9, 1.
33. McAuley, K. B.; MacGregor, J. F.; Hamielec, A. E. AIChE J 1990, 36, 837.
34. Frank, H. P. Österreich Chem-Z 1967, 68, 360.
35. Muñoz-Escalona, A.; Hidalgo, G.; Lafuente, P.; Martinez Núñez, M. F.; Méndez, L.; Michels, W.; Peña, B.; Sancho, J. In Proceedings of 5th International Congress on Metallocene Polymers, 1998; p 73.
36. Bergström, C.; Väänänen, T. L. J.; Seppälä, J. J Appl Polym Sci 1997, 63, 1071.
37. Sernetz, F. G.; Mülhaupt, R. J Polym Sci Part A Polym Chem 1997, 35, 2549–2560.